Simple closed-form solution to predict short-range surface plasmons in thin films bounded by asymmetric media and its application to hole arrays

IEEE Photonics Journal
An IEEE Photonics Society Publication

Open Access

Simple Closed-Form Solution to Predict Short-Range Surface Plasmons in Thin Films Bounded by Asymmetric Media and Its Application to Hole Arrays

Volume 8, Number 1, February 2016

M. Lorente-Crespo, Student Member, IEEE
C. Mateo-Segura, Member, IEEE

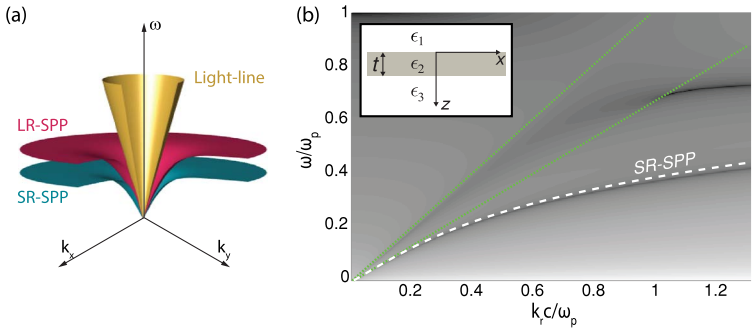

DOI: 10.1109/JPHOT.2016.2521267
1943-0655 © 2016 IEEE

IEEE photonics SOCIETY

IEEE

Simple Closed-Form Solution to Predict Short-Range Surface Plasmons in Thin Films Bounded by Asymmetric Media and Its Application to Hole Arrays

M. Lorente-Crespo, *Student Member, IEEE*, and C. Mateo-Segura, *Member, IEEE*

Institute of Sensors, Signals and Systems, Heriot-Watt University, Edinburgh EH14 4AS, U.K.

DOI: 10.1109/JPHOT.2016.2521267

Manuscript received December 2, 2015; revised January 18, 2016; accepted January 19, 2016. Date of publication January 27, 2016; date of current version February 3, 2016. This work was supported by the FP7 DORADA Project under Grant IAPP-2013-610691. Corresponding author: M. Lorente-Crespo (e-mail: ml343@hw.ac.uk).

Abstract: Thin metallic films bounded by two dielectric media can support long- and short-range surface plasmon polaritons (SPPs). The dispersion relation associated with these hybrid modes is given by a complex transcendental equation that can only be solved numerically. In this paper, a simple approximate analytical solution for the short-range modes is derived. To validate the proposed analytical solution, short-range SPPs in a 2-D periodic array of small holes are studied and compared to full-wave simulations. The results prove a spectral response in excellent agreement.

Index Terms: Plasmonics, nanohole arrays, theory and design.

1. Introduction

Metallo-dielectric interfaces can support bounded modes associated with collective charge oscillations that propagate along the interface and are confined to its vicinity: surface plasmon polaritons (SPPs). If two semi-infinite media are considered, the dispersion relation of the SPPs is well known [1]. This dispersion relation may be dramatically different when considering a bounded thin finite metal film instead [2]. In this configuration, if the thickness is smaller than the attenuation length, coupling between the SPPs on the upper and lower interfaces results in the formation of two hybrid modes with thickness-dependent dispersion relation and opposite field distributions termed the long-range (LR-) SPP and the short-range (SR-) SPP. For thick films, these modes become degenerate and the dispersion relation in this case tends towards that of the SPP of a single flat interface [1].

In the present work, a finite thin film of thickness t and complex permittivity ϵ_2 bounded by semi-infinite dielectric media of real permittivity ϵ_1 and ϵ_3 is considered; see the inset of Fig. 1(a). The associated dispersion relation in this case shows a complex behavior and cannot be solved analytically. For the symmetric case $(\epsilon_1 = \epsilon_3)$, the LR- and SR- modes can be studied separately [1]. An approximate solution for the LR-SPPs dispersion relation can be found in [3]. However, a simple closed-form solution to analyze SR-SPPs has yet to appear. If such a solution is to be available, the spectral position of SR-SPP resonances could be readily obtained. These resonances have been recently exploited in a wide variety of applications [4]–[8]. For instance, it has been recently reported that SR-SPPs play a key role in extraordinary optical transmission (EOT),

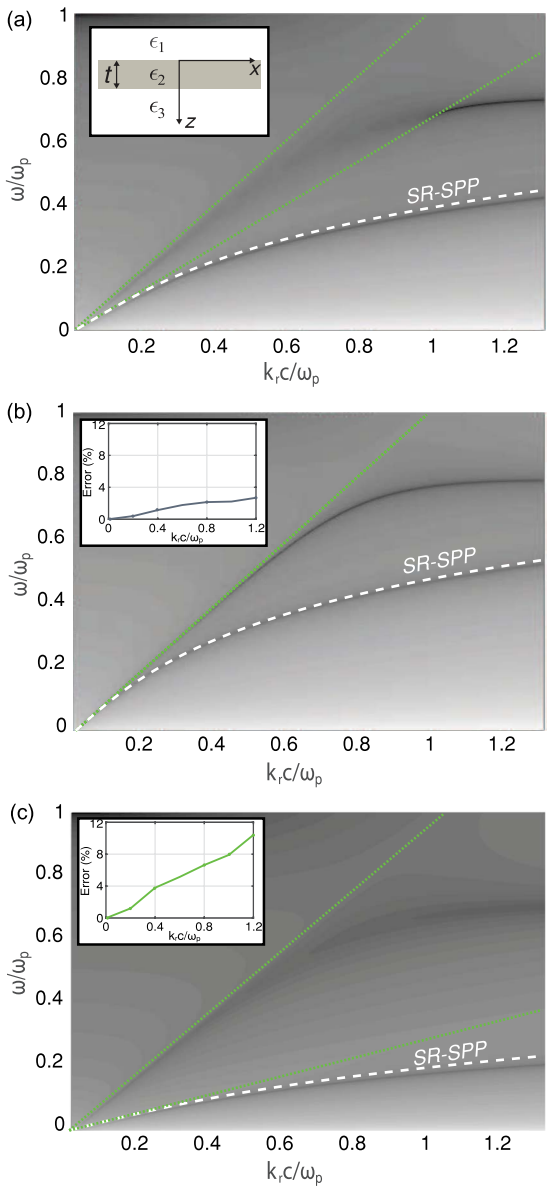

Fig. 1. Dispersion relation of a 15-nm-thick silver film (gray scale) when the film is (a) sandwiched between dielectrics with $\epsilon_1 = 2.25$ and $\epsilon_3 = 1$, (b) free-standing ($\epsilon_1 = \epsilon_3 = 1$), and (c) when $\epsilon_1 = 11$ and $\epsilon_3 = 1$. Darker colors correspond to lower values of the dispersion. The light lines in the different dielectrics are shown as green dotted lines. The approximate solution for the SR-SPP is indicated by the white dashed line. Inset (a): Metallic film with thickness t and permittivity ϵ_2 sandwiched between two semi-infinite dielectric media with permittivities ϵ_1 and ϵ_3. Inset (b) and (c): Percentage deviation from the numerical solution in each case.

as well as in the design of absorbers [9], polarizers [10], or color filters [11], [12]. Likewise, they have also shown promise in biosensing [13] and for implementing plasmonic waveguides [14]. Therefore, the solution proposed in this work has the potential to significantly simplify and speed-up the design process of these devices while providing an intuitive understanding of the effect of the geometry on the excitation of these plasmons.

2. Propagation Constant of Short-Range Plasmons in Asymmetric Environments

In the following and without loss of generality, the example presented in the inset of Fig. 1(a) where the layers are parallel to the x axis is considered. The out-of-plane direction, which refers

to the direction perpendicular to the interface, is z. Since SPPs are transverse magnetic (TM) in nature [1], they are better described by their in-plane magnetic field component H_y

$$H_y = H_0 f(z) \exp[i(\omega t - k_x x)] \tag{1}$$

where k_x is the in-plane complex propagation constant, H_0 is a normalization constant, and the propagation is assumed to be along x. The term $f(z)$ describes the z dependence of the magnetic field so that it exponentially decays with increasing distance to the interfaces. Using Maxwell equations, the non-zero components of the electric field are

$$E_x = \frac{i}{\omega \epsilon_0 \epsilon} \frac{dH_y}{dz} \tag{2}$$

$$E_z = -\frac{k_x}{\omega \epsilon_0 \epsilon} H_y. \tag{3}$$

The tangential components of the magnetic field must be continuous at the interfaces. Therefore, $f(z)$ can be written as [15]

$$f(z) = \begin{cases} \exp[k_{z_1} z], & z < 0 \\ \cosh(k_{z_2} z) + \frac{k_{z_1} \epsilon_m}{k_{z_2} \epsilon_1} \sinh(k_{z_2} z), & 0 > z > t \\ \left[\cosh(k_{z_2} t) + \frac{k_{z_1} \epsilon_m}{k_{z_2} \epsilon_1} \sin(k_{z_2} t)\right] \exp[-k_{z_3}(z - t)], & z > t \end{cases} \tag{4}$$

where k_{z_j} with $j = 1$, 2, and 3 are the wavevectors in the different media and fulfill the equality

$$k_{z_j}^2 = k_x^2 - \epsilon_j k_0^2. \tag{5}$$

Forcing continuity of the tangential electric component, the following dispersion relation is obtained [15]

$$\tanh(k_{z_2} t)\left(\epsilon_1 \epsilon_3 k_{z_2}^2 + \epsilon_2^2 k_{z_1} k_{z_3}\right) = -k_{z_2} \epsilon_2 (\epsilon_1 k_{z_3} + \epsilon_3 k_{z_1}). \tag{6}$$

This transcendental equation can only be solved numerically. If the thickness is small enough so that $|k_{z_2} t| \ll 1$, by means of a Taylor series expansion up to first order, the hyperbolic tangent in (6) can be simplified to

$$k_{z_2} t\left(\epsilon_1 \epsilon_3 k_{z_2}^2 + \epsilon_2^2 k_{z_1} k_{z_3}\right) = -k_{z_2} \epsilon_2 (\epsilon_1 k_{z_3} + \epsilon_3 k_{z_1}). \tag{7}$$

For a fixed frequency, the propagation constant of the SR-SPP is far smaller than that of the SPP of each single flat interface

$$k_{x_j}^{\mathrm{SPP}} = k_0 \left(\frac{\epsilon_2 \epsilon_j}{\epsilon_2 + \epsilon_j}\right)^{\frac{1}{2}}, \quad j = 1, 3. \tag{8}$$

That is, SR-SPPs satisfy the inequality $k_x \ll k_{x_j}^{SPP}$ for $j = 1$, 3. This inequality can be expressed as $k_{z_2}/\epsilon_2 \ll k_{z_j}/\epsilon_j$. As a result, the first term of the left hand side of (7) becomes negligible and (7) can be reduced to

$$t \epsilon_2^2 k_{z_1} k_{z_3} = -\epsilon_2 (\epsilon_1 k_{z_3} + \epsilon_3 k_{z_1}). \tag{9}$$

A similar reasoning can be applied to the LR-SPPs, where the term $\epsilon_1 \epsilon_3 k_{z_2}^2$ may be neglected.

Assuming $\epsilon_1 \neq \epsilon_3$, the wavevector in medium 3 can be written as a function of that in medium 1, i.e.,

$$k_{z_3} = \sqrt{k_{z_1}^2 + k_0^2 \Delta} \tag{10}$$

where $\Delta = \epsilon_1 - \epsilon_3$ may take any real value. In this sense, (9) can be expressed as a function of a single variable, k_{z_1}. Additionally, if $|k_0^2\Delta/k_{z_1}^2| < 1$, a further simplification of the square root in (10) can be performed by means of a Taylor series expansion up to first order. Subsequently, a monic cubic equation (11), shown in the following, with coefficients $p = (2\epsilon_1 - \Delta)/(t\epsilon_2)$, $q = k_0^2\Delta/2$, and $r = k_0^2\Delta\epsilon_1/(2t\epsilon_2)$ is obtained:

$$k_{z_1}^3 + pk_{z_1}^2 + qk_{z_1} + r = 0. \tag{11}$$

Such an equation can be solved analytically by means of the cubic formula. The associated root corresponding to the SR-SPP is given by

$$k_{z_1}^{\mathrm{SR}} = -\frac{p}{3} + A - \frac{3q - p^2}{9A} \tag{12}$$

where

$$A = \frac{(-2p^3 + 9pq - 27r + B)^{\frac{1}{3}}}{3\sqrt{[3]2}} \tag{13}$$

$$B = 3\sqrt{3}(-p^2q^2 + 4q^3 + 4p^3r - 18pqr + 27r^2)^{\frac{1}{2}}. \tag{14}$$

The complex propagation constant of the SR-SPPs can be obtained by simple combination of (5) and (12)

$$k_x^{\mathrm{SR}} = \left[\left(k_{z_1}^{\mathrm{SR}}\right)^2 + \epsilon_1\left(\frac{\omega}{c}\right)^2\right]^{\frac{1}{2}}. \tag{15}$$

3. Numerical Example: Short-Range Plasmons of a Thin Silver Film

Next, a numerical example is studied. The dispersion relation of a $t = 15$ nm silver film in the real $k - \omega$ plane when a vacuum superstrate $(\epsilon_3 = 1)$ and a glass substrate are considered $(\epsilon_1 = 2.25)$ is depicted in Fig. 1(a). Additionally, the free-standing case $(\epsilon_1 = \epsilon_3 = 1)$ is shown in Fig. 1(b), and a higher contrast case ($\epsilon_3 = 1$ and $\epsilon_1 = 11$) in Fig. 1(c). Silver's complex dielectric permittivity is described using a Drude's model with $\epsilon_\infty = 1$, plasma frequency $\omega_p = 1.37\times 10^{16}$ rad/s, and damping frequency $\omega_c = 2.5 \times 10^{14}$ rad/s [16]. For the sake of comparison, the approximate solution of the dispersion relation of the SR-SPP according to (12)–(15) appears superimposed to the numerical solution of (6). In the short-k range, the agreement is excellent for both the asymmetric $(\epsilon_1 \neq \epsilon_3)$ and the symmetric $(\epsilon_1 = \epsilon_3)$ environments, even when the contrast is as high as $\Delta = 10$. The second mode arising at higher frequencies corresponds to the LR-SPP. The dispersion curves of both the LR- and SR-SPPs lie at the right of the light-lines. These modes cannot be directly excited by normally incident light impinging from the dielectrics because of their larger propagation constant [1], as is well known. The required extra momentum can be provided via grating coupling [17], as in the example considered later in this paper. To further evaluate the accuracy of the derived closed-form, the insets of Fig. 1(b) and (c) show the percentage deviation of the approximate analytical solution from that obtained by numerically solving (6) in each case. Small discrepancies arise towards the long-k range, where $|k_{z_2}t| \ll 1$ is not perfectly fulfilled. The maximum error, which corresponds to the case $\Delta = 10$ is below 11%.

The symmetric case, as shown in Fig. 1(b), is merely an special case of the most general asymmetric configuration. In this scenario, the dispersion relation can be directly obtained by simplification of the cubic equation (equating Δ to zero); (11) becomes linear and the solution simplifies to

$$k_{z_1}^{\mathrm{SR}} = \frac{-2\epsilon_1}{t\epsilon_2}. \tag{16}$$

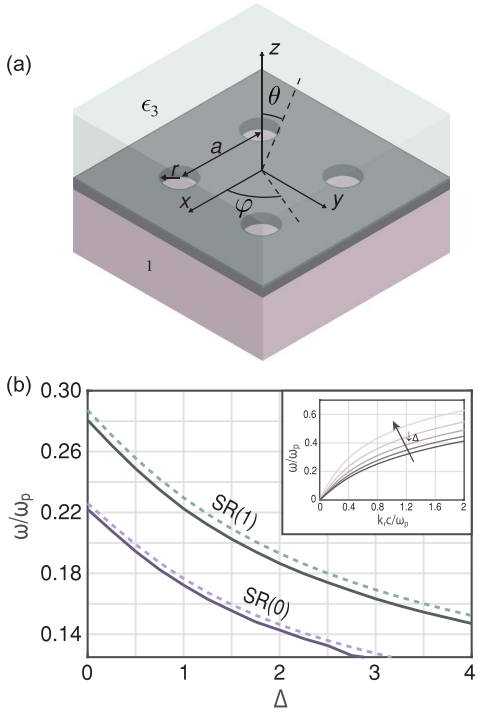

Fig. 2. (a) Proposed geometry. The plane-wave impinges from $-\hat{z}$. (b) Closed-form (dashed lines) and simulated (solid lines) resonance frequencies of the lower order modes when the superstrate is vacuum ($\epsilon_3 = 1$) and the contrast between this and the substrate is $\Delta = 0$–4. The geometrical parameters are $t = 15$ nm, $r = 20$ nm, and $a = 500$ nm. (Inset) Approximate dispersion relation of the SR-SPP mode for $\Delta = 0$–4. Lighter shades correspond to smaller contrasts.

As in the asymmetric case, the wavevector can be substituted in (15) to obtain the propagation constant of the SR-SPPs, Fig. 1(b). Note that (16) agrees with that reported by Raether in [1] after approximating the hyperbolic tangent by its Taylor expansion.

4. Application to Hole-Arrays

As an application example of the proposed closed-form, a square grating of subwavelength circular apertures with radius $r = 20$ nm and periodicity $a = 500$ nm perforated in a $t = 15$ nm film is considered; see Fig. 2(a). Such periodic array imparts the necessary additional momentum to the impinging light for the excitation of SPPs yet supports the propagation of SR-SPPs. The in-plane component of the momentum is $|k_{\|}| = |(k_{L_x} \pm nG)\hat{x} + (k_{L_y} \pm mG)\hat{y}|$, where $G = 2\pi/a$ is the reciprocal lattice constant, and k_{L_x} and k_{L_y} are the x and y components of the incident light momentum. Considering that the equality $k_x = k_{\|}$ must be satisfied in order to excite SPPs, and that (12) holds, the frequencies at which an incoming TM polarized plane wave will couple to the SR-SPPs can be obtained analytically by the solution of the two simultaneous equations. To illustrate this, Fig. 2(b) shows the resonant frequencies of the two lower order SR-modes for different permittivity contrasts Δ, maintaining $\epsilon_3 = 1$. To validate the approximation, the SR-SPP resonances calculated using (12)–(15) are super-imposed to the simulated ones. The simulated resonant frequencies are obtained from the spectral position of the absorption maxima as given by CST Microwave Studio. Absorption is calculated as $1 - T - R$, where T and R stand for zero-order transmission and reflection, respectively. The cut-off frequency of the holes can be calculated as in [18] by simply exchanging the roles of the dielectric and the metal. For $r = 20$ nm empty holes, $\omega_{co}/\omega_p = 1.62$, which is far above the upper frequency limit considered here. Therefore, the holes do not support any propagating modes.

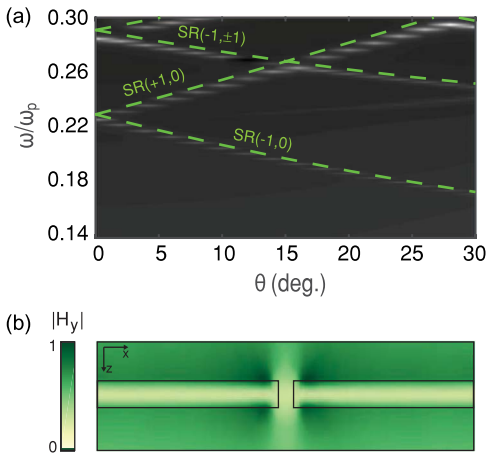

Fig. 3. (a) Simulated angular absorption spectra at the $\varphi = 0^\circ$ plane. Lighter colors correspond to higher values of absorption. The superimposed green lines indicate the theoretical resonance frequencies of the (n, m) order SR-SPPs. (b) Normalized $|H_y|$ distribution at the xz plane for $\omega/\omega_p = 0.22$ and normal incidence. (a), (b) $t = 15$ nm, $a = 500$ nm, and $r = 20$ nm.

Thus, it is reasonable to consider them as weak scatterers. As shown in Fig. 2(b), the derived solution predicts accurately the spectral position of the absorption peaks independently of the permittivity contrast between both surrounding dielectric media. Increasing the contrast leads to a red-shift on the mode resonances, which can be explained by looking at the inset of Fig. 2(b). There, it can be seen how for a fixed propagation constant, higher Δ results in the mode arising at lower frequencies.

The same 2-D square grating is subsequently embedded in a symmetric environment $(\epsilon_1 = \epsilon_3)$. Such configuration can be experimentally realized by fabricating symmetric samples or, more commonly, including index matching liquids [19]–[21]. Fig. 3(a) shows the simulated angular absorption spectra when a plane wave is impinging from $(\varphi = 0^\circ, \theta = 0 - 30^\circ)$. There, it can be observed that the derived solution is also accurate in the case of oblique illumination. Owing to the oblique incidence, there is an extra in-plane component to the wavevector and the SR-SPPs hybridize into even and odd order modes, as shown in the scattering spectra. To verify that the excited SPP is indeed the SR-SPP, Fig. 3(b) shows the magnitude of the parallel component of the magnetic field, H_y, normalized to its maximum at $\omega/\omega_p = 0.22$ and normal incidence. As expected for the SR-SPPs, H_y exhibits a zero distribution inside the metal film.

Thus far, any effects due to the holes, other than providing a mechanism for the excitation of SPPs, have been neglected. The effect of increasing the size of the apertures is investigated in Fig. 4(a). As it can be seen, for larger holes, the simulations increasingly deviate from the theory due to the limited validity of the empty lattice approximation. The red-shift of the resonances with respect to the predictions has been extensively studied in the literature [22]–[24] and is out of the scope of this work.

The thickness of the metal film plays a key role in the dispersion relation of thin films and thus, in the excitation of SR-SPPs. Moreover, the approximation derived in this work is thickness-dependent and remains valid as long as $|k_{z_2} t| \ll 1$. Therefore, the estimated spectral position where resonance occurs is more accurate for thinner films, as confirmed by Fig. 4(b). Above a critical thickness, the SR and LR-SPPs are uncoupled and converge to the SPP mode of the single interface, as in (8), which is not well described by (16). To illustrate this, the dispersion relation given by (6) is solved for a $t = 300$ nm film. The predicted normalized dispersion curve of the SR-SPP according to (16) and that of the single interface appear superimposed to the numerical solution of (6) in Fig. 4(c). The LR- and SR-SPPs are degenerate in this case, and (8) is more accurate for describing the overall behavior.

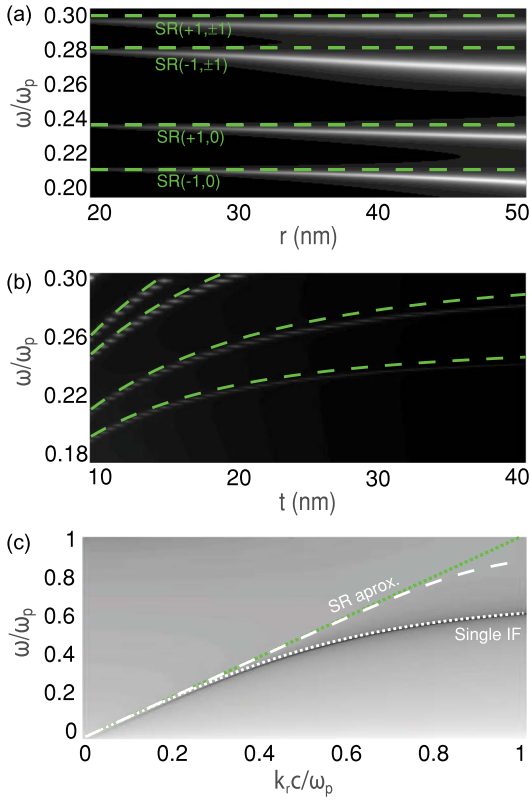

Fig. 4. Absorption at ($\varphi = 0°$, $\theta = 5°$) incidence for a grating with $a = 500$ nm (a) vs. hole radius when $t = 15$ nm and (b) vs. film thickness when $r = 20$ nm. The predicted dispersion curves are shown as green dashed lines. (c) Dispersion relation of a 300-nm-thick silver film. The light line is shown as a green dotted line. The approximate solution is indicated by the white dashed line and that of the single interface by the white dotted line.

5. Conclusion

In conclusion, we derived a simple expression for calculating the dispersion relation of SR-SPPs in both symmetric and asymmetric dielectric media configurations. The proposed closed-form can be used to predict the associated resonances of this type of modes and hence ease the design of SR-SPPs based applications. The dispersion curves estimated with the proposed approximation and those obtained when solving the transcendental equation for finite metal slabs find an excellent agreement in the short-k region. To further explore the accuracy of this approach a 2-D lattice of subwavelength holes was considered. Within the empty lattice approximation limitations, the estimated and simulated resonant frequencies are in very good agreement for normal and oblique incident light. Our solution remains valid as long as $|k_{z_2} t| \ll 1$. Above a critical thickness, the SR- and LR- modes become degenerate and the dispersion curves converge to that of a single smooth interface, as suggested by the simulations.

Acknowledgment

The authors wish to thank C. García-Meca and G. C. Ballesteros for valuable input and suggestions.

References

[1] H. Raether, *Surface Plasmons on Smooth and Rough Surfaces and on Gratings*. Berlin, Germany: Springer-Verlag, 1988.
[2] E. Economou, "Surface plasmons in thin films," *Phys. Rev.*, vol. 182, no. 2, p. 539, Jun. 1969.

[3] F. Yang, J. Sambles, and G. Bradberry, "Long-range surface modes supported by thin films," *Phys. Rev. B*, vol. 44, no. 11, p. 5855, Sep. 1991.
[4] S. Xiao and N. A. Mortensen, "Surface-plasmon-polariton-induced suppressed transmission through ultrathin metal disk arrays," *Opt. Lett.*, vol. 36, no. 1, pp. 37–39, Jan. 2011.
[5] Y. Alaverdyan, B. Sepúlveda, L. Eurenius, E. Olsson, and M. Käll, "Optical antennas based on coupled nanoholes in thin metal films," *Nature Phys.*, vol. 3, no. 12, pp. 884–889, Nov. 2007.
[6] S. G. Rodrigo *et al.*, "Extraordinary optical transmission through hole arrays in optically thin metal films," *Opt. Lett.*, vol. 34, no. 1, pp. 4–6, Jan. 2009.
[7] B. Zeng, Y. Gao, and F. J. Bartoli, "Ultrathin nanostructured metals for highly transmissive plasmonic subtractive color filters," *Sci. Rep.*, vol. 3, p. 2840, Oct. 2013.
[8] B. Zeng, Z. H. Kafafi, and F. J. Bartoli, *Transparent Conducting Electrodes based on 1D and 2D Ag Nanogratings for Organic Photovoltaics*, ArXiv e-prints, Dec. 2014.
[9] W. Bai *et al.*, "Broadband short-range surface plasmon structures for absorption enhancement in organic photovoltaics," *Opt. Exp.*, vol. 18, pp. 620–630, Nov. 2010.
[10] J. Braun, B. Gompf, G. Kobiela, and M. Dressel, "How holes can obscure the view: Suppressed transmission through an ultrathin metal film by a subwavelength hole array," *Phys. Rev. Lett.*, vol. 103, no. 20, Nov. 2009, Art. ID 203901.
[11] L. Sun *et al.*, "Influence of structural parameters to polarization-independent color-filter behavior in ultrathin Ag films," *Opt. Commun.*, vol. 333, pp. 16–21, Dec. 2014.
[12] L. B. Sun *et al.*, "Effect of relative nanohole position on colour purity of ultrathin plasmonic subtractive colour filters," *Nanotechnol.*, vol. 26, no. 30, Jul. 2015, Art. ID 305204.
[13] R. Wan, F. Liu, and Y. Huang, "Ultrathin layer sensing based on hybrid coupler with short-range surface plasmon polariton and dielectric waveguide," *Opt. Lett.*, vol. 35, no. 2, pp. 244–246, Jan. 2010.
[14] R. Wan, F. Liu, X. Tang, Y. Huang, and J. Peng, "Vertical coupling between short range surface plasmon polariton mode and dielectric waveguide mode," *Appl. Phys. Lett.*, vol. 94, no. 14, Apr. 2009, Art. ID 141104.
[15] J. Burke, G. I. Stegeman, and T. Tamir, "Surface-polariton like waves guided by thin, lossy metal films," *Phys. Rev. B Condens. Matter*, vol. 33, no. 8, Apr. 1986, pp. 5186–5201.
[16] P. Johnson and R. Christy, "Optical constants of the noble metals," *Phys. Rev. B*, vol. 6, no. 12, p. 4370, Dec. 1972.
[17] R. H. Ritchie, E. T. Arakawa, J. J. Cowan, and R. N. Hamm, "Surface-plasmon resonance effect in grating diffraction," *Phys. Rev. Lett.*, vol. 21, no. 22, pp. 1530–1533, Nov. 1968.
[18] C. Pfeiffer, E. Economou, and K. Ngai, "Surface polaritons in a circularly cylindrical interface: Surface plasmons," *Phys. Rev. B*, vol. 10, no. 8, p. 3038, Oct. 1974.
[19] A. Krishnan *et al.*, "Evanescently coupled resonance in surface plasmon enhanced transmission," *Opt. Commun.*, vol. 200, no. 1–6, pp. 1–7, 2001.
[20] L. Pang, K. A. Tetz, and Y. Fainman, "Observation of the splitting of degenerate surface plasmon polariton modes in a two-dimensional metallic nanohole array," *Appl. Phys. Lett.*, vol. 90, no. 11, Mar. 2007, Art. ID 111103.
[21] M. J. A. de Dood, E. F. C. Driessen, D. Stolwijk, and M. P. van Exter, "Observation of coupling between surface plasmons in index-matched hole arrays," *Phys. Rev. B*, vol. 77, p. 115437, Mar. 2008.
[22] H. Lezec and T. Thio, "Diffracted evanescent wave model for enhanced and suppressed optical transmission through subwavelength hole arrays," *Opt. Exp.*, vol. 12, no. 16, pp. 3629–3651, Aug. 2004.
[23] D. Pacifici, H. J. Lezec, L. A. Sweatlock, R. J. Walters, and H. A. Atwater, "Universal optical transmission features in periodic and quasiperiodic hole arrays," *Opt. Exp.*, vol. 16, no. 12, pp. 9222–9238, Jun. 2008.
[24] H. Liu and P. Lalanne, "Microscopic theory of the extraordinary optical transmission," *Nature*, vol. 452, no. 7188, pp. 728–731, Apr. 2008.